Supplementary Information

An Ultrathin Cobalt-Iron Oxide Catalyst for Water Oxidation on Nanostructured Hematite Photoanodes

Laurent Liardet,[1] Jordan E. Katz,[1,2] Jingshan Luo,[3,4] Michael Grätzel[3] and Xile Hu,[1,*]

[1] Laboratory of Inorganic Synthesis and Catalysis, Institute of Chemical Sciences and Engineering, École Polytechnique Fédérale de Lausanne (EPFL), ISIC-LSCI, 1015 Lausanne, Switzerland

[2] Department of Chemistry and Biochemistry, Denison University, 100 W. College St., Granville, OH 43023, USA

[3] Laboratory of Photonics and Interfaces, Institute of Chemical Sciences and Engineering, École Polytechnique Fédérale de Lausanne (EPFL), ISIC-LPI, 1015 Lausanne, Switzerland

[4] Institute of Photoelectronic Thin Film Devices and Technology, College of Electronic Information and Optical Engineering, Nankai University, Tianjin 300350, China

Table S1. Comparison of different hematite photoanodes coated with cobalt-based catalysts and reported performances under AM 1.5 illumination (100 mW cm^{-2}).

Materials	Hematite synthesis	Catalyst deposition	Electrolyte	potential [V Vs RHE]	J [mA cm^{-2}]@ 1.0 V vs RHE	J [mA cm^{-2}]@ 1.23 V vs RHE	Ref.
$Fe_2O_3/Al_2O_3/CoFeO_X$	APCVD	Photo-electrodeposition	1 M KOH	0.8	1.6	2.5	This work
Ti:Fe_2O_3 nanorod array/$CoFeO_x$	Hydrothermal	Spin coating	1 M KOH	0.8	0.6	2.5	*1*
Fe_2O_3 dendrite-carbon nitride composite/$CoFeO_x$	Hydrothermal	Electrodeposition	1 M NaOH	1.0	/	0.6	*2*
Inverse opal Fe_2O_3/CoO_x	ALD	ALD	0.1 M KOH	1.0	/	1.0	3
Sn:Fe_2O_3/CoO_x nanowires	Hydrothermal	Electrodeposition	1 M KOH	0.4	0.5	2.2	*4*
Pt:Fe_2O_3/Co-Pi wormlike structure	Hydrothermal	Photo-electrodeposition	1 M NaOH	0.7	2.4	4.3	*5*
P:Fe_2O_3/Co-Pi nanowires	Hydrothermal	Photo-electrodeposition	1 M NaOH	0.8	1.5	3.1	*6*

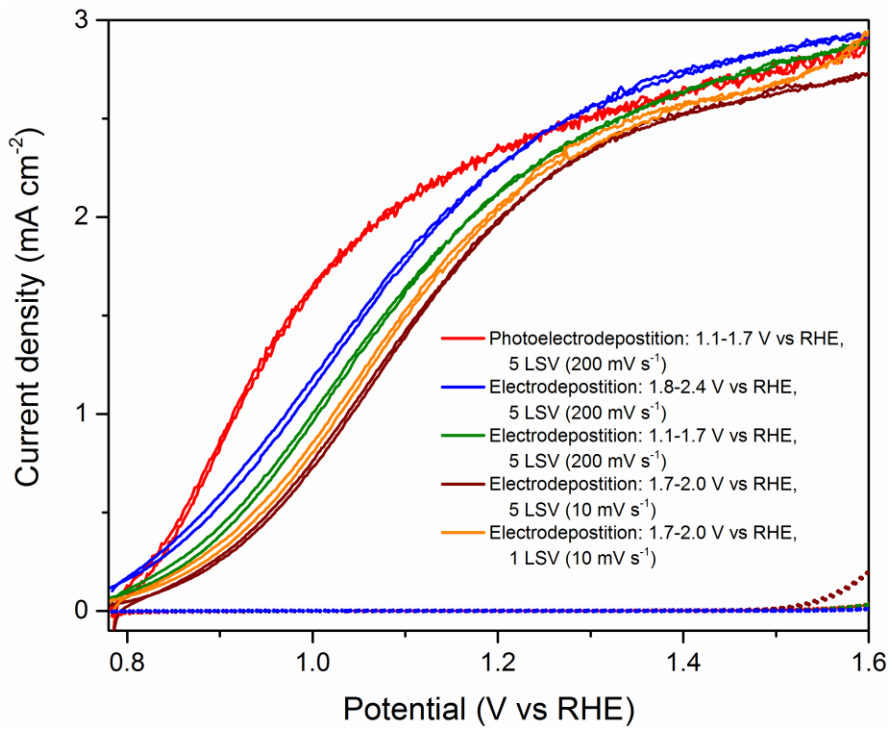

Fig. S1. Polarization curves of hematite photoanodes in 1 M KOH under illumination coated with $CoFeO_x$ photoelectrodeposited and electrodeposited by different conditions.

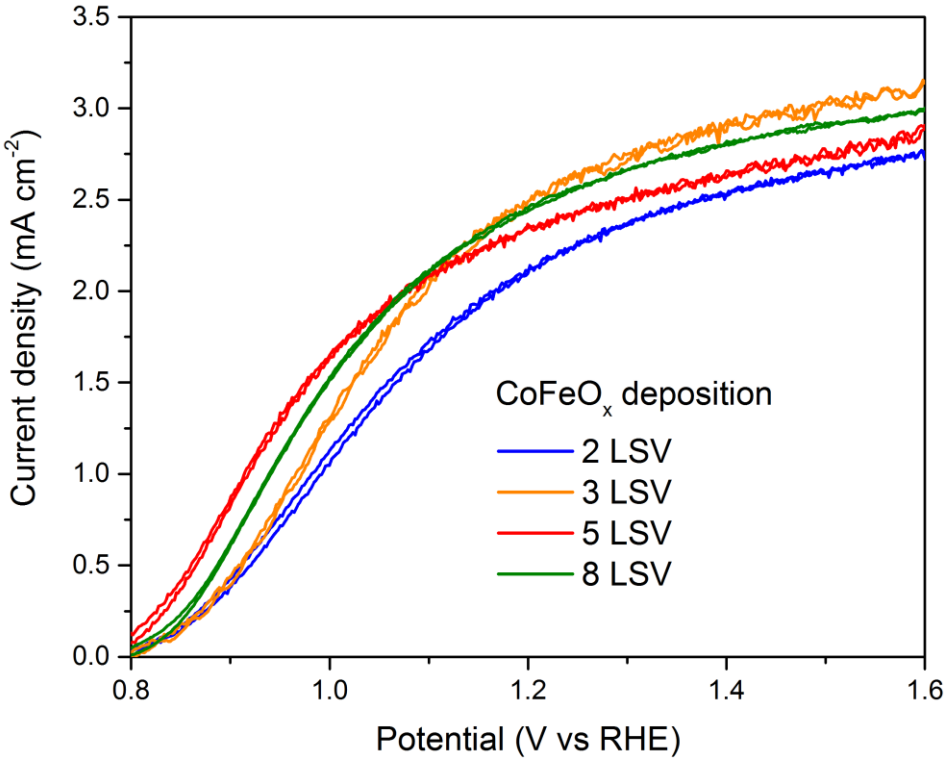

Fig. S2. Polarization curves of hematite photoanodes coated with $CoFeO_x$ with different number of linear sweeps, measured under simulated AM1.5 illumination in 1 M KOH and showing the best photocurrent onset potential when $CoFeO_x$ is deposited with 5 linear sweeps. Scan rate 10 mV s^{-1}.

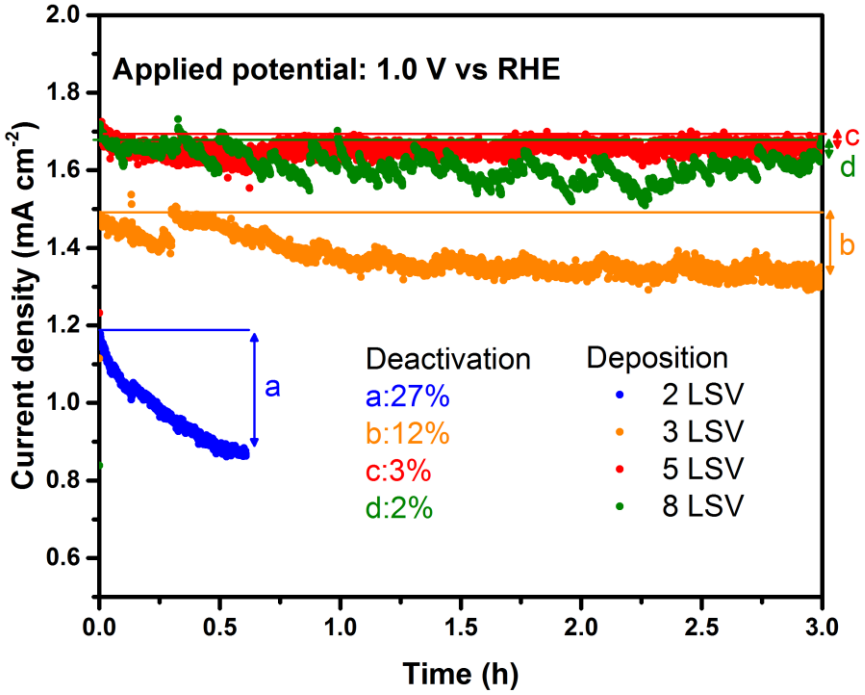

Fig. S3. Constant potential electrolysis in 1 M KOH at 1.0 V vs RHE under simulated AM1.5 illumination of hematite photoanodes coated with $CoFeO_x$ deposited with different number of linear sweeps, showing the photocurrent stability increases when $CoFeO_x$ is deposited with higher numbers of linear sweeps.

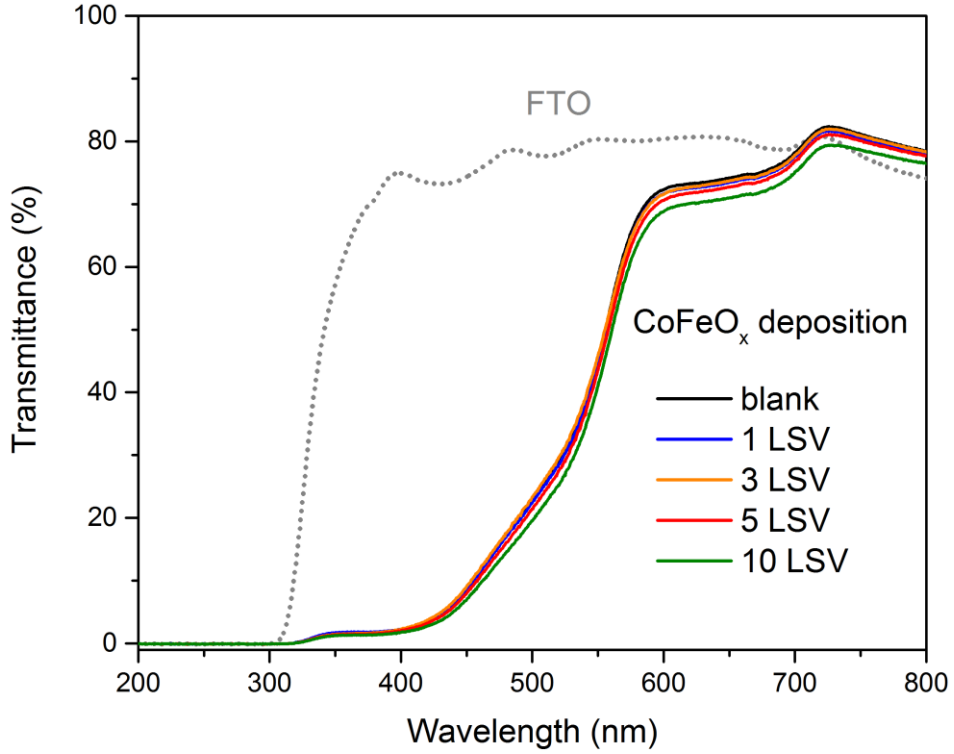

Fig. S4. Transmittance of the fluorine-doped tin-oxide (FTO) substrate as well as hematite photoanodes, uncoated and coated with $CoFeO_x$ deposited with different numbers of LSV sweeps, indicating the optical transparency of the $CoFeO_x$ layer.

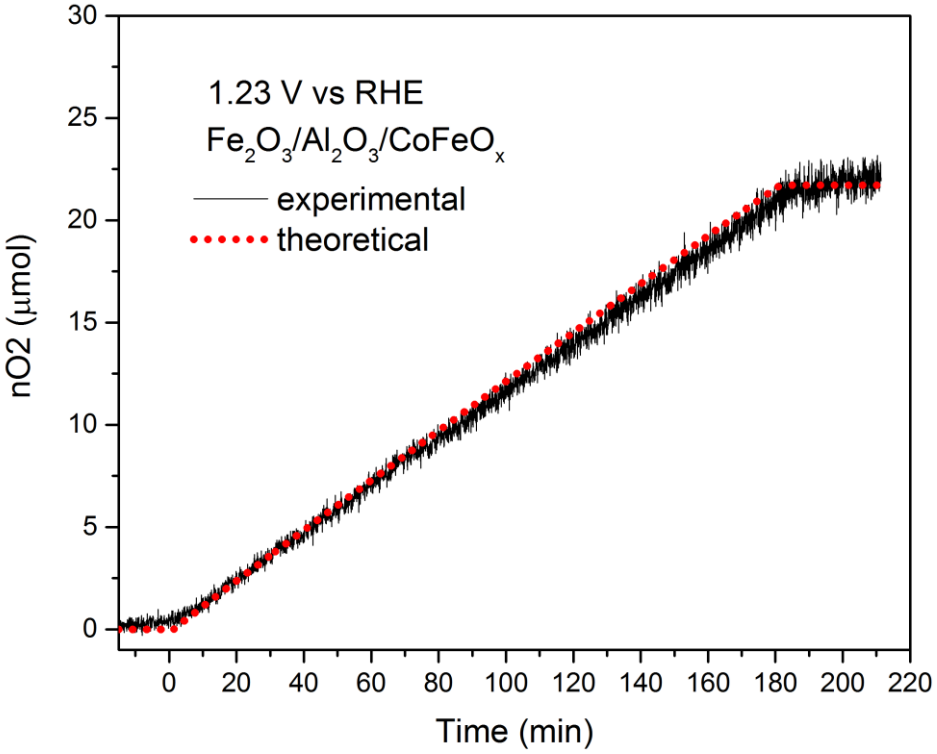

Fig. S5. Measured and predicted number of moles of O_2 produced by the $CoFeO_x$-coated hematite photoanode over time under illumination at 1.23 V vs RHE, showing that nearly 100% faradaic efficiency is obtained.

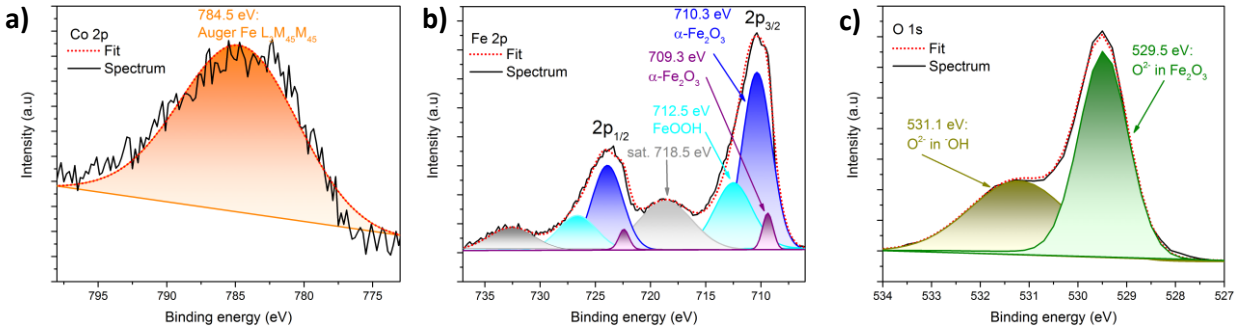

Fig. S6. XPS spectra of blank hematite with high-resolution spectra of a) Co 2p region, b) Fe 2p region and c) O 1s region.

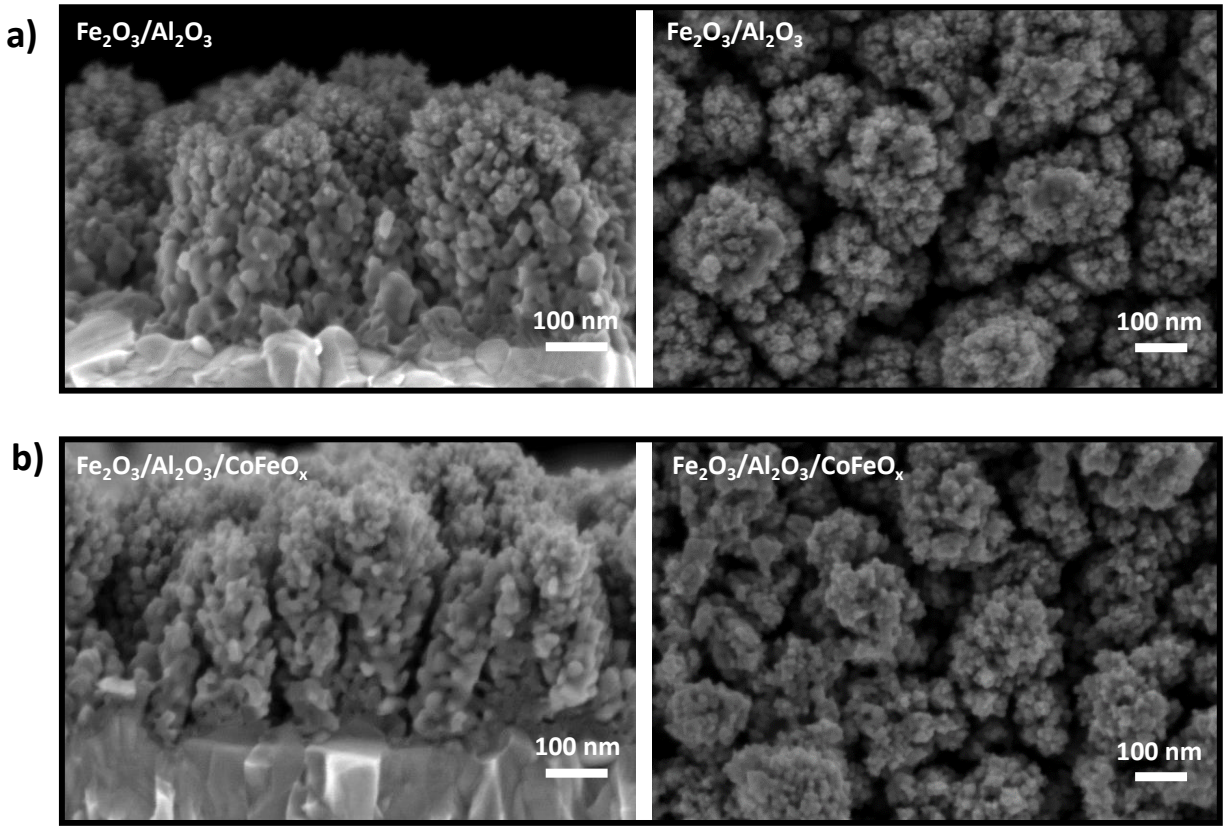

Fig. S7. SEM images showing cross-section and top-down views of a) catalyst-free hematite and b) $CoFeO_x$-coated hematite, showing no morphological changes after deposition of $CoFeO_x$.

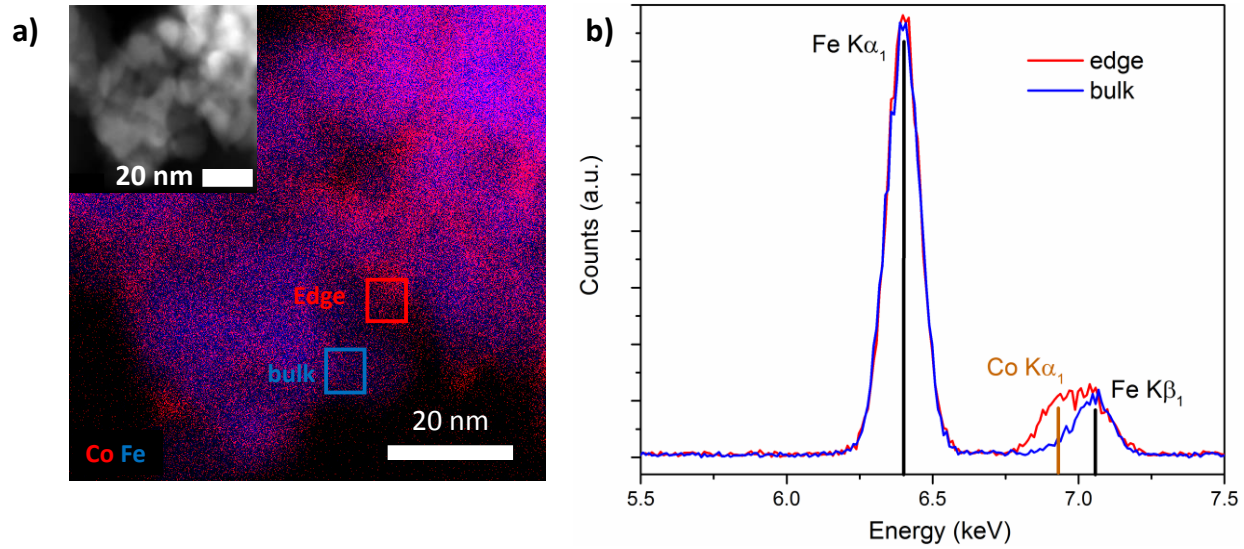

Fig. S8. a) STEM-EDX image of hematite coated with 10 LSV of $CoFeO_x$ (inset HAADF image). b) EDX spectrum of the bulk region (blue square in a)) and of the edge region (red square in a)), indicating an increase of Co concentration on the edge of the particle.

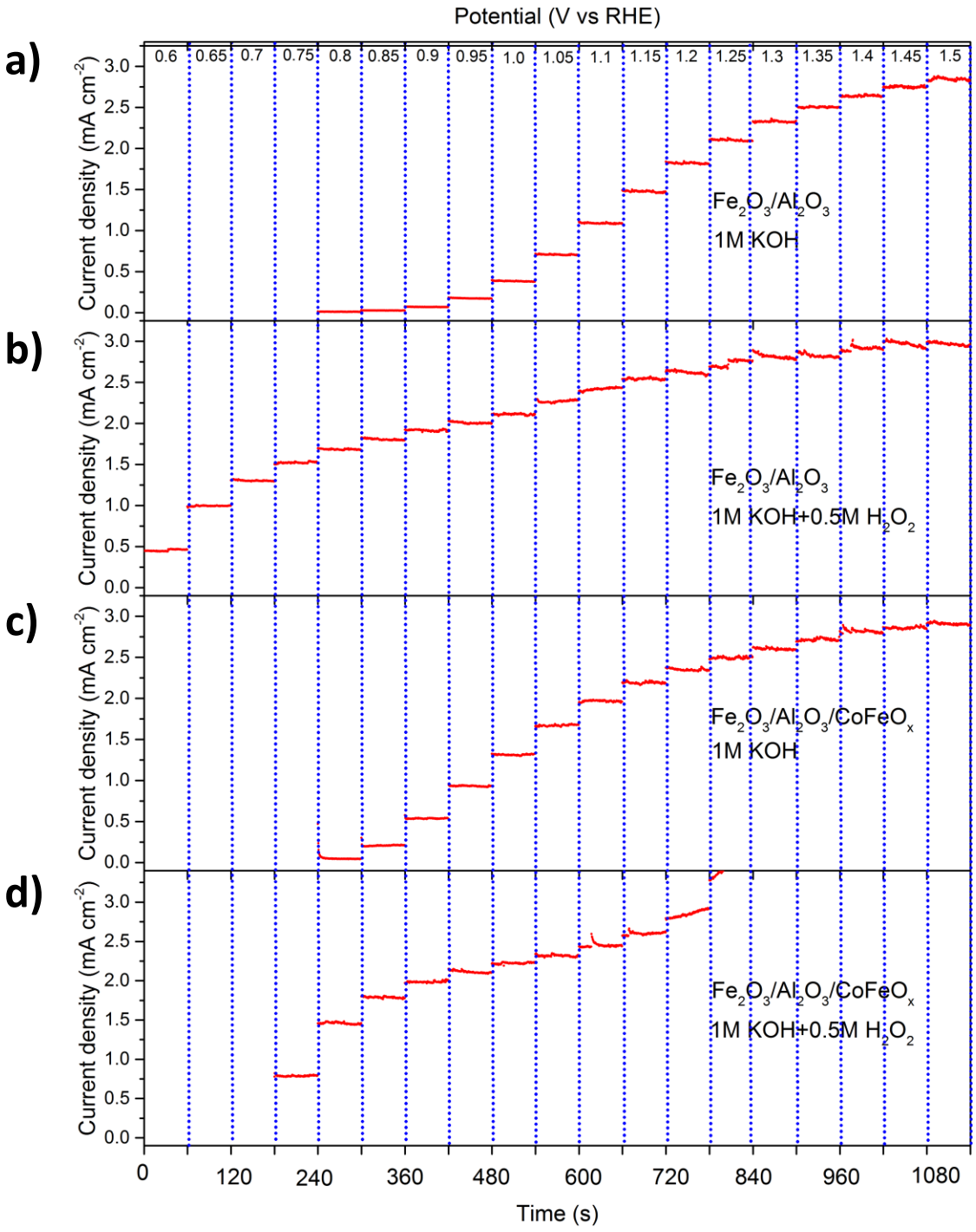

Fig. S9. Steady-state photocurrents measured by chronoamperometry between 0.6 and 1.5 V vs RHE of Fe_2O_3/Al_2O_3 and $Fe_2O_3/Al_2O_3/CoFeO_x$ in 1 M KOH (a and c) and in 1 M KOH + 0.5 M H_2O_2 (b and d).

Calculation of the charge injection and separation efficiencies

The experimentally measured photocurrent can be obtained from Equation 1. J_{photo} is defined as the theoretical maximum photocurrent density (J_{max}) that can be obtained from the hematite photoanode multiplied by the charge separation and charge injection efficiencies (η_{sep} and η_{inj}, respectively). The value of J_{max} was previously determined as 10.9 mA cm^{-2} and corresponds to the integration of the absorption spectrum of a typical APCVD hematite electrode use here with the AM 1.5G solar spectrum (100 mW cm^{-2}).[7]

$$J_{photo} = J_{max} \times \eta_{sep} \times \eta_{inj} \quad (1)$$

The experimental photocurrent in 1 M KOH (J_{photo}(KOH)) is obtained with a similar equation (Equation 2).

$$J_{photo}(\mathrm{KOH}) = J_{max} \times \eta_{sep} \times \eta_{inj} \quad (2)$$

In Equation 3, for J_{photo}(KOH + H_2O_2), the charge injection efficiency can be neglected (η_{inj} = 1) since H_2O_2 is known to be a highly efficient hole scavenger, effectively collecting every photogenerated hole that reaches the semiconductor/electrolyte interface.[7]

$$J_{photo}(\mathrm{KOH} + \mathrm{H_2O_2}) = J_{max} \times \eta_{sep} \quad (3)$$

From Equations 2 and 3, η_{sep} and η_{inj} can be obtained by simple rearrangement and substitution, giving Equations 4 and 5.

$$\eta_{inj} = \frac{J_{photo}(\mathrm{KOH})}{J_{photo}(\mathrm{KOH} + \mathrm{H_2O_2})} \quad (4)$$

$$\eta_{sep} = \frac{J_{photo}(\mathrm{KOH} + \mathrm{H_2O_2})}{J_{max}} \quad (5)$$

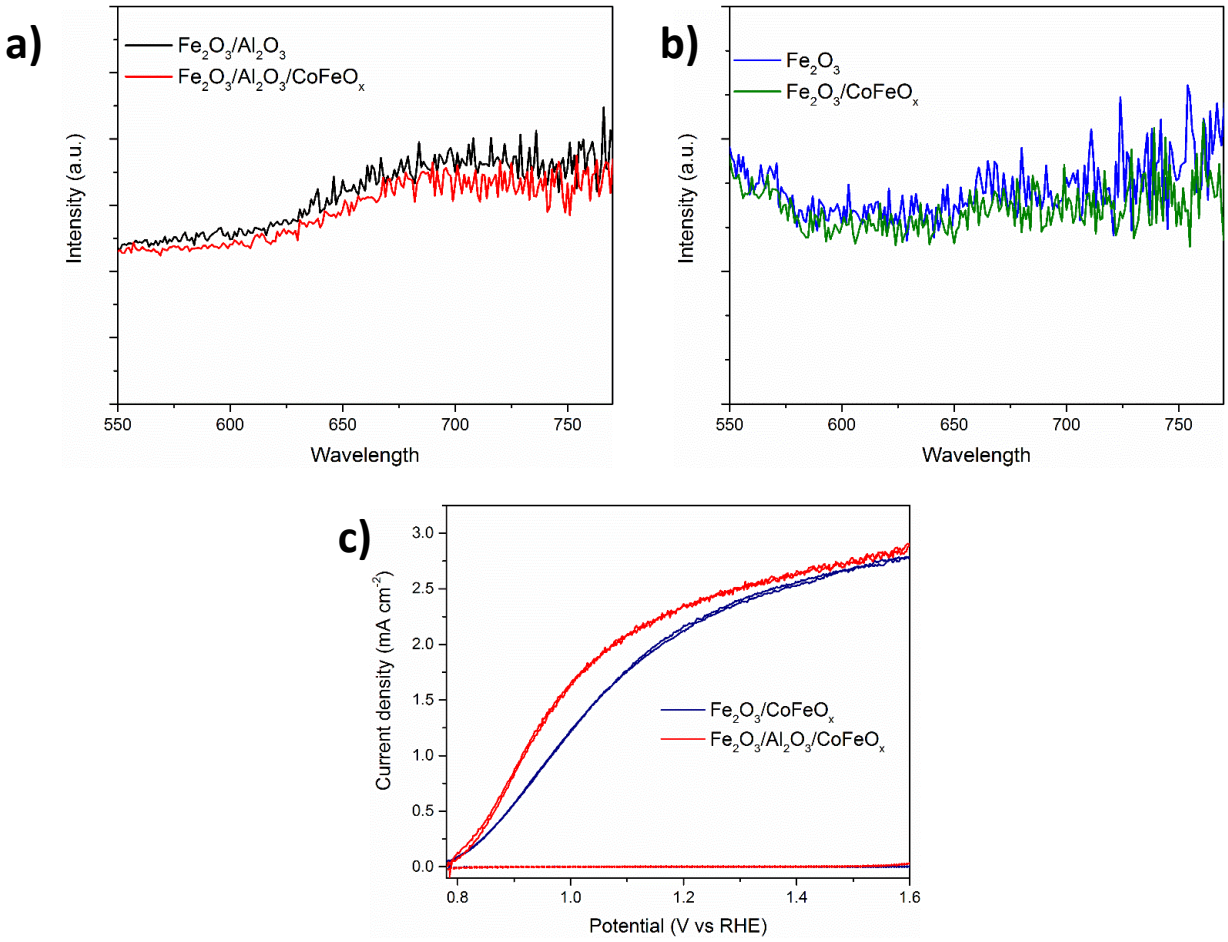

Fig. S10. a) Photoluminescence emission spectra of catalyst-free and $CoFeO_x$-coated hematite photoanodes with Al_2O_3 and b) without Al_2O_3. c) Polarization curves in 1 M KOH under illumination (lines) and in the dark (dotted lines) of $CoFeO_x$-coated hematite with and without Al_2O_3, showing a difference of fill factor when Al_2O_3 is present or not.

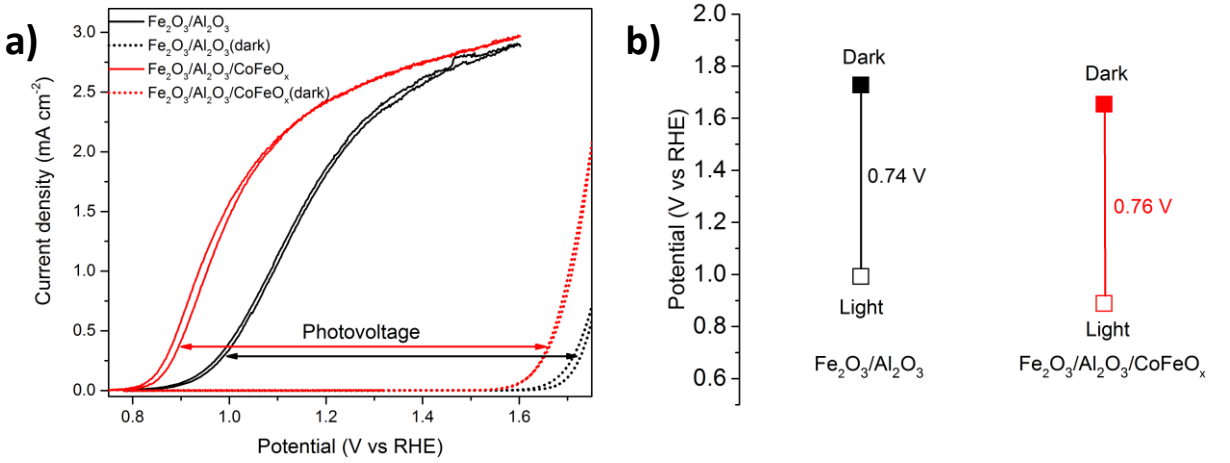

Fig. S11. a) Polarization curves in 1 M KOH under illumination and in the dark of catalyst-free and $CoFeO_x$-coated hematite and b) corresponding extracted photovoltages for each.

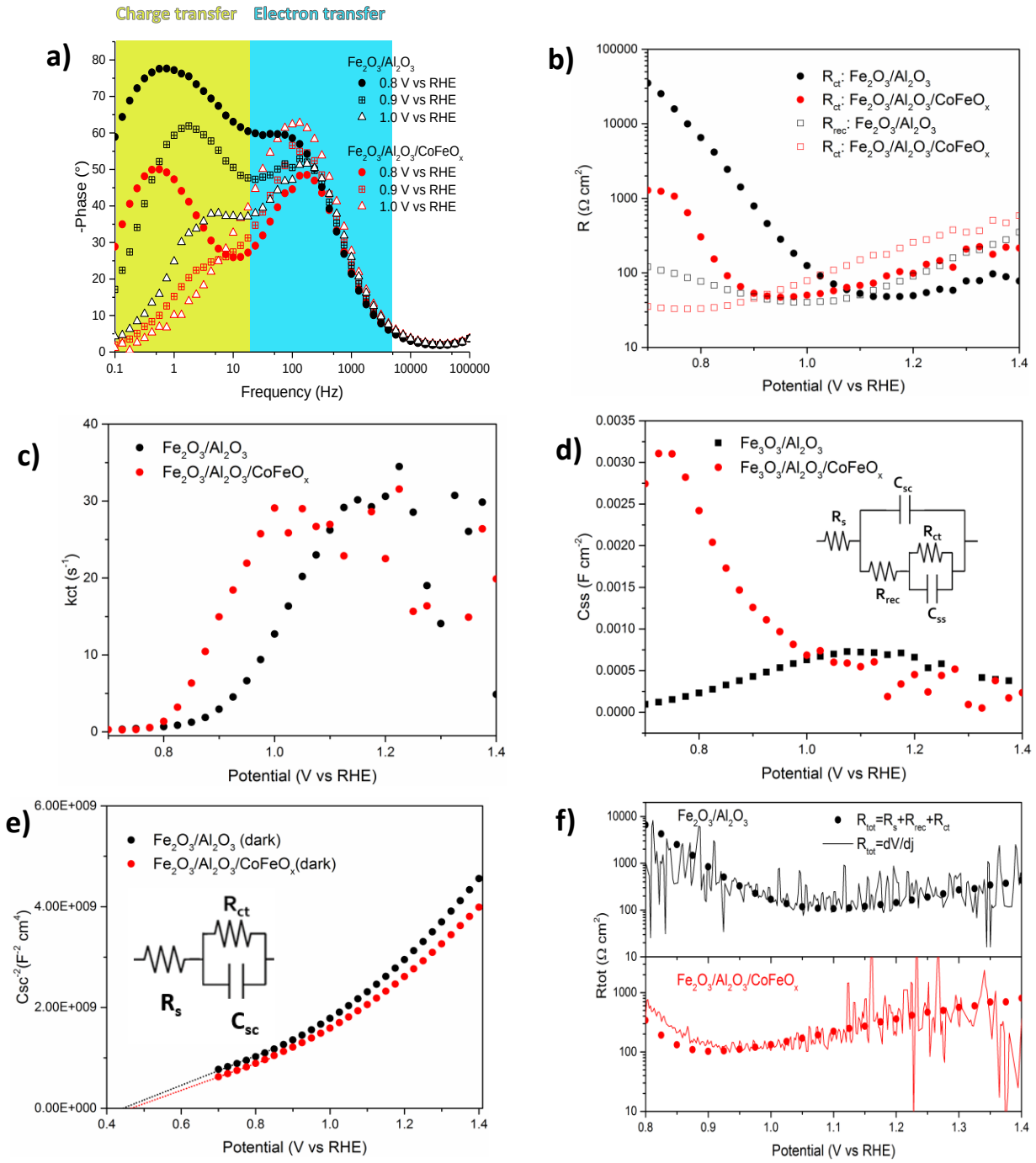

Fig. S12. a) Bode plot of Fe_2O_3/Al_2O_3 and $Fe_2O_3/Al_2O_3/CoFeO_x$ at different potentials, showing the potential-dependent phase change in the charge transfer frequency region. b) Resistance to charge transfer (R_{ct}) and resistance to recombination (R_{rec}) of Fe_2O_3/Al_2O_3 and $Fe_2O_3/Al_2O_3/CoFeO_x$ at different potentials under illumination. c) Charge transfer rate constant (k_{ct}) at different potentials for Fe_2O_3/Al_2O_3 and $Fe_2O_3/Al_2O_3/CoFeO_x$ under illumination. d) Capacitance of surface states at different applied potentials of Fe_2O_3/Al_2O_3 and $Fe_2O_3/Al_2O_3/CoFeO_x$, indicating an increase of capacitance when $CoFeO_x$ is deposited. e) Mott-Schottky plot of Fe_2O_3/Al_2O_3 and $Fe_2O_3/Al_2O_3/CoFeO_x$ in the dark, showing a negligible change of the flat band potential after deposition of $CoFeO_x$. d) Comparison of the total resistance from impedance fits and from the derivative of the photocurrent as a function of the applied potential, demonstrating good agreement between the two methods.

References

1 **Xu, Y.-F., Wang, X.-D., Chen, H.-Y., Kuang, D.-B. & Su, C.-Y. Toward High Performance Photoelectrochemical Water Oxidation: Combined Effects of Ultrafine Cobalt Iron Oxide Nanoparticle. *Advanced Functional Materials* 26, 4414-4421, doi:doi:10.1002/adfm.201600232 (2016).**

2 **Bhandary, N., Singh, A. P., Ingole, P. P. & Basu, S. Enhancing the Photoelectrochemical Performance of a Hematite Dendrite/Graphitic Carbon Nitride Nanocomposite through Surface Modification with CoFeOx. *ChemPhotoChem* 1, 70-75, doi:doi:10.1002/cptc.201600008 (2017).**

3 **Riha, S. C. *et al.* Atomic Layer Deposition of a Submonolayer Catalyst for the Enhanced Photoelectrochemical Performance of Water Oxidation with Hematite. *ACS Nano* 7, 2396-2405 (2013).**

4 **Li, M. *et al.* Morphology and Doping Engineering of Sn-Doped Hematite Nanowire Photoanodes. *Nano Letters* 17, 2490-2495, doi:10.1021/acs.nanolett.7b00184 (2017).**

5 **Kim, J. Y. *et al.* Single-crystalline, wormlike hematite photoanodes for efficient solar water splitting. *Scientific Reports* 3, 2681, doi:10.1038/srep02681 (2013)**

6 **Zhang, Y. *et al.* Nonmetal P-doped hematite photoanode with enhanced electron mobility and high water oxidation activity. *Energy & Environmental Science* 8, 1231-1236, doi:10.1039/C4EE03803G (2015).**

7 **Dotan, H., Sivula, K., Gratzel, M., Rothschild, A. & Warren, S. C. Probing the photoelectrochemical properties of hematite ([small alpha]-Fe2O3) electrodes using hydrogen peroxide as a hole scavenger. *Energy & Environmental Science* 4, 958-964, doi:10.1039/C0EE00570C (2011).**